Long-range propagation of finite-amplitude acoustic waves in an ocean waveguide

Kaëlig Castor,[a] Peter Gerstoft, Philippe Roux, and W. A. Kuperman
Marine Physical Laboratory, University of California San Diego, La Jolla, California 92093-0238

B. E. McDonald[b]
Naval Research Laboratory, Acoustics Division, Washington D.C. 20375

(Received 3 November 2003; revised 5 April 2004; accepted 5 April 2004)

A hybrid method coupling nonlinear and linear propagation codes is used to study the nonlinear signature of long-range acoustic propagation for high-amplitude sources in an ocean waveguide. The differences between linear and nonlinear propagation are investigated in deep and shallow water environments. The spectral reshaping that occurs in nonlinear propagation induces two main effects: in shallow water, an unusual arrival time structure in the lowest order modes is observed, and in both shallow and deep water environments, there is a tendency to have acoustic energy more uniformly distributed across modes. Further, parametric low-frequency generation in deep water is a candidate for the coupling between water and sediments for T-wave formation. [DOI: 10.1121/1.1756613]

PACS numbers: 43.30.Lz, 43.30.Bp, 43.30.Qd, 43.25.Cb. [AIT] Pages: 2004–2010

I. INTRODUCTION

Our goal in this paper is to study how to characterize acoustic signals generated by a high intensity source and propagated over several thousand kilometers in an ocean waveguide.[1,2] In a high-energy event, such as an explosive shock wave, nonlinear processes induce changes in the ocean's acoustic properties. The nonlinear signature of an acoustic waveform propagated over long ranges is investigated in this paper.

Several approaches have been put forward to model explosion waveforms and to estimate source levels.[3–6] In this article we do not deal with the phenomena that occur directly at the source. The simulations presented here use a narrow-band source in order to focus on signal evolution during nonlinear propagation over very long ranges. Two propagation models are used here. First, a time–domain code based on the Nonlinear Progressive Wave Equation (NPE)[7] is used to propagate a finite-amplitude acoustic wave field. Second, this code is coupled to the linear KRAKEN[8] normal mode code to propagate this field over very long oceanic paths beyond a certain distance for which the amplitude of the acoustic field is sufficiently low.

The results in this paper show that an initially high-amplitude acoustic wave retains a nonlinear signature, characteristic of its nonlinear origin, after becoming linear and propagating over great distances. One of the significant transformations that occurs during nonlinear propagation and still remains at very long ranges is in the waveform spectrum. The spectrum modification is associated with a frequency–mode coupling that is an energy redistribution upon both modes and frequencies during propagation. This frequency–mode coupling leads to a particular shape in the modal structure in terms of arrival time and energy distribution. Two types of long-range paths are analyzed in deep water that correspond respectively to a source located in shallow or deep water. Other results to be demonstrated are the following.

(1) Nonlinear effects are smaller in deep water than in shallow water due to the higher geometrical spreading that strongly diminishes the amplitude.
(2) In deep water, a nonlinear signature is characterized by energy more uniformly spread out over a large number of modes. In shallow water, this redistribution can be clearly observed, but fewer modes are excited.
(3) Nonlinearity in shallow water can be high enough to strongly alter the modal dispersion and thus change the arrival time of the modes.
(4) Nonlinear frequency–mode coupling can be responsible for an acoustic coupling from the earth to the SOFAR channel, which for long-range propagation is commonly designated as a T wave. Indeed, low parametric frequency excitation in deep water, that can be restricted in shallow water because of the waveguide cutoff frequency, gives rise to lower-order mode excitation. These lower modes are spread over the water column, and therefore a strong interaction with the bottom can contribute to an increased sea/bottom coupling.

In Sec. II, the NPE model used in the simulations is presented. In Sec. III we will present, for a narrow-band source, the nonlinear spectrum reshaping during nonlinear propagation, and then its effect on modal dispersion, by pointing out the differences due to the environment. Finally, the low-order mode excitation due to the low parametric frequency generated in deep water will be examined because of its possible influence on T-wave formation.

[a]Electronic mail: kaelig.castor@cea.fr
[b]Electronic mail: mcdonald@sonar.nrl.navy.mil

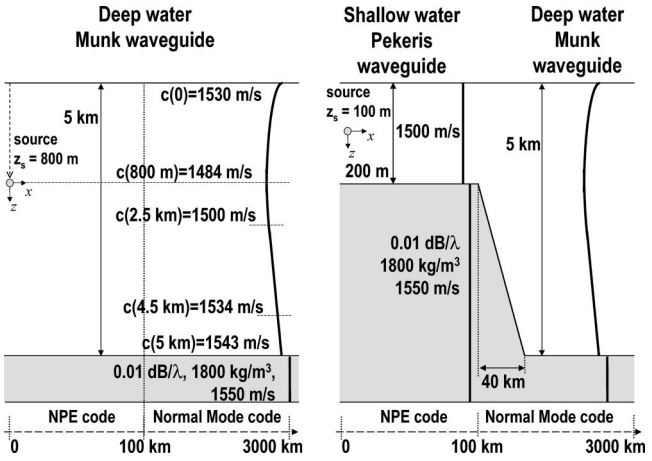

FIG. 1. Schematic diagrams of the environments used in this work.

II. EQUATIONS OF NONLINEAR ACOUSTICS AND WEAK SHOCK PROPAGATION

The NPE was developed by McDonald and Kuperman[7,9,10] to compute a time–domain solution for the acoustic field in a waveguide, including dominant nonlinear effects. The model is derived from the Euler equations of fluid dynamics retaining lowest-order nonlinearity augmented by an adiabatic equation of state relating pressure and density. The NPE is cast in a wave-following coordinate system moving at a nominal average sound speed c_0 in the longitudinal propagation direction x. The NPE describes nonlinear propagation of compression waves in the time–domain and is expressed as

$$\frac{\partial p}{\partial t} = -\frac{c_0}{2}\int_{\infty}^{x}\nabla_{\perp}^2 p\, dx - \frac{\partial}{\partial x}\left(c_1 p + \frac{\beta}{2\rho_0 c_0}p^2\right) + \frac{\delta}{2}\frac{\partial^2 p}{\partial x^2}, \tag{1}$$

where p is the acoustic pressure, and subscript 0 denotes ambient values. The constants δ and β are thermoviscous absorption and nonlinearity parameters ($\beta = 3.5$ for water), c_1 is the environmental sound speed fluctuation about c_0. One can reformulate a similar NPE[7,11] in terms of a dimensionless overdensity variable $R = p/(\rho_0 c_0^2)$, and the initial source amplitude is referred as the maximum overdensity R_m in the following. The terms on the right-hand side of Eq. (1) represent from left to right, diffraction, refraction, nonlinear steepening, and thermoviscous dissipation. Since the attenuation of low-frequency sound (<1 kHz) in seawater is very small, the thermoviscous dissipation term in the NPE is neglected here. However, a porous medium attenuation,[12] which is approximately linear in frequency, is included in the sediment layer adding at the right-hand side of Eq. (1), a quasi-Cauchy integral expressed as

$$0.02\alpha\frac{c_0}{2}\int_0^{\infty}\frac{\partial_x p(x+x')}{x'+\Delta x}dx', \tag{2}$$

where Δx and α are, respectively, the x grid spacing and attenuation in dB/wavelength (Fig. 1).

Recently, the well-known KZK[13,14] equation has been expressed in a form similar to the NPE. Thus, to simulate sonic boom propagation through a turbulent atmosphere, Blanc-Benon *et al.*[15] developed a modified KZK expressed as

$$\frac{\partial p}{\partial x} = \frac{c_0}{2}\int_{-\infty}^{t}\nabla_{\perp}^2 p\, dt + \frac{1}{c_0^2}\frac{\partial}{\partial t}\left(c_1 p + \frac{\beta}{2\rho_0 c_0}p^2\right) + \frac{\delta}{2c_0^3}\frac{\partial^2 p}{\partial t^2}. \tag{3}$$

This KZK equation includes the refractive term that accounts for the environmental variation of the sound speed. The NPE, Eq. (1), and KZK, Eq. (3), formulations are similar with the roles of time and distance reversed ($x_{\mathrm{NPE}} = -c_0 t_{\mathrm{KZK}}; t_{\mathrm{NPE}} = t_{\mathrm{KZK}} + x_{\mathrm{KZK}}/c_0$).[16] The differences between both approaches are only in the numerical algorithms. The KZK uses classical finite difference schemes for all the calculations while the NPE uses an accurate scheme to calculate the refraction and nonlinear steepening terms: a second-order upwind flux corrected transport scheme[17] that accounts properly for shock dissipation automatically avoiding Gibbs' oscillations without the necessity of adding an artificial attenuation like in a classical finite difference scheme.

III. LONG-RANGE NONLINEAR PROPAGATION OF A NARROWBAND SOURCE

A. Nonlinear effects on spectral evolution

The quadratic nonlinearity in Eq. (1) implies that the nonlinear contribution to the local sound speed is $\beta p/(\rho_0 c_0)$. In nonlinear propagation, the acoustic energy losses are increased for high initial amplitudes because of shock dissipation. When the shock wave discontinuity begins, a cascade of higher frequencies is generated. This phenomenon increases entropy locally and constitutes a mechanism of energy dissipation, even in a perfect fluid. The shock wave formation distance decreases as the source level increases.[18] Thus, for a strong explosion, dissipation at the shock front leads to a high rate of energy decay and amplitude saturation of the signal propagated in the waveguide.

The nonlinear propagation of an acoustic wave induces a spectral reshaping due to harmonic generation. Nonlinear propagation of two primary monochromatic waves at frequencies f_1 and f_2 gives rise to induced secondary radiation at frequencies $f_1 \pm f_2$. These secondary waves alter the spectrum of the acoustic field. The sum and difference frequencies are generated by parametric interaction, which has been studied for a long time,[19] especially in tomographic applications,[20,21] and more recently to measure the nonlinear parameter β in liquids.[22] Generally, radiation of sum- and difference-frequency sound from the nonlinear interaction region formed by the intersection of nonplanar modes in the waveguide is referred to as scattering of sound by sound.[18]

The NPE code is initialized by a sine-wave packet, modulated by Gaussian envelopes having scale sizes 600 m in range and 150 m in depth, and centered at the frequency $f = 30$ Hz. Two propagation environments are studied here (Fig. 1). In the first case [Fig. 1(a)], the source is located in shallow water, at a source depth $z_s = 100$ m. The second case

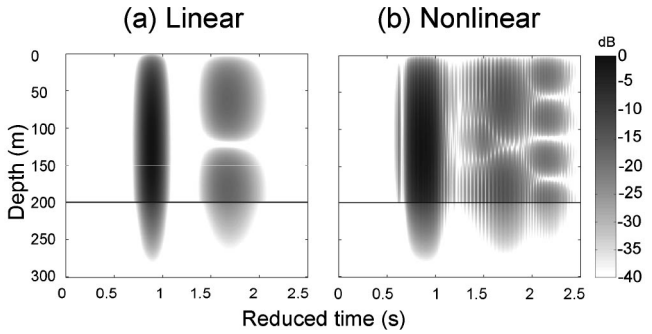

FIG. 2. Time series envelopes in shallow water at 100-km range, for a narrowband source centered at $f_c = 30$ Hz, at 100 m depth, with a maximum overdensity $R_m = 1 \times 10^{-5}$ (a. linear case) and $R_m = 5 \times 10^{-3}$ (b. nonlinear case).

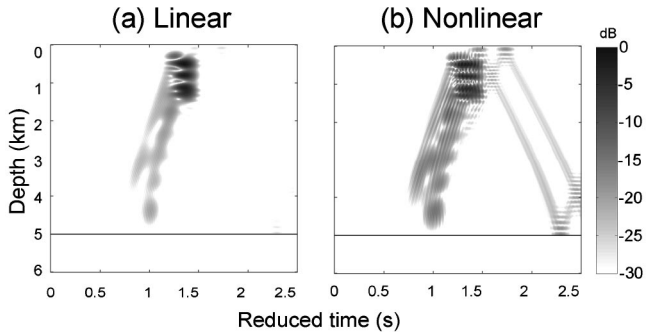

FIG. 3. Time series envelopes in deep water at 100-km range, for a narrowband source centered at $f_c = 30$ Hz, at 800 m depth, with a maximum overdensity $R_m = 1 \times 10^{-5}$ (a. linear case) and $R_m = 5 \times 10^{-3}$ (b. nonlinear case).

studied [Fig. 1(b)] is when the source is placed in deep water, in the middle of the SOFAR channel ($z_s = 800$ m). In both cases, the nonlinear propagation using the NPE code is carried to the 100-km range. Figure 2 and Fig. 3 give the time series envelopes at the 100-km range, resulting from the stated initial conditions. Figure 4 displays the depth-averaged spectrum of the source and at the 100-km range in shallow and deep water. After propagation over the 100-km range, the higher frequencies are damped out and only the first harmonic remains important in both cases. In deep water, the spectrum displays a low-frequency peak near 2–5 Hz due to nonlinear effects that lead to an energy transfer toward all the difference frequency components during propagation. So, this parametric difference frequency wave (DFW) at low frequency is directly related to the source frequency band-

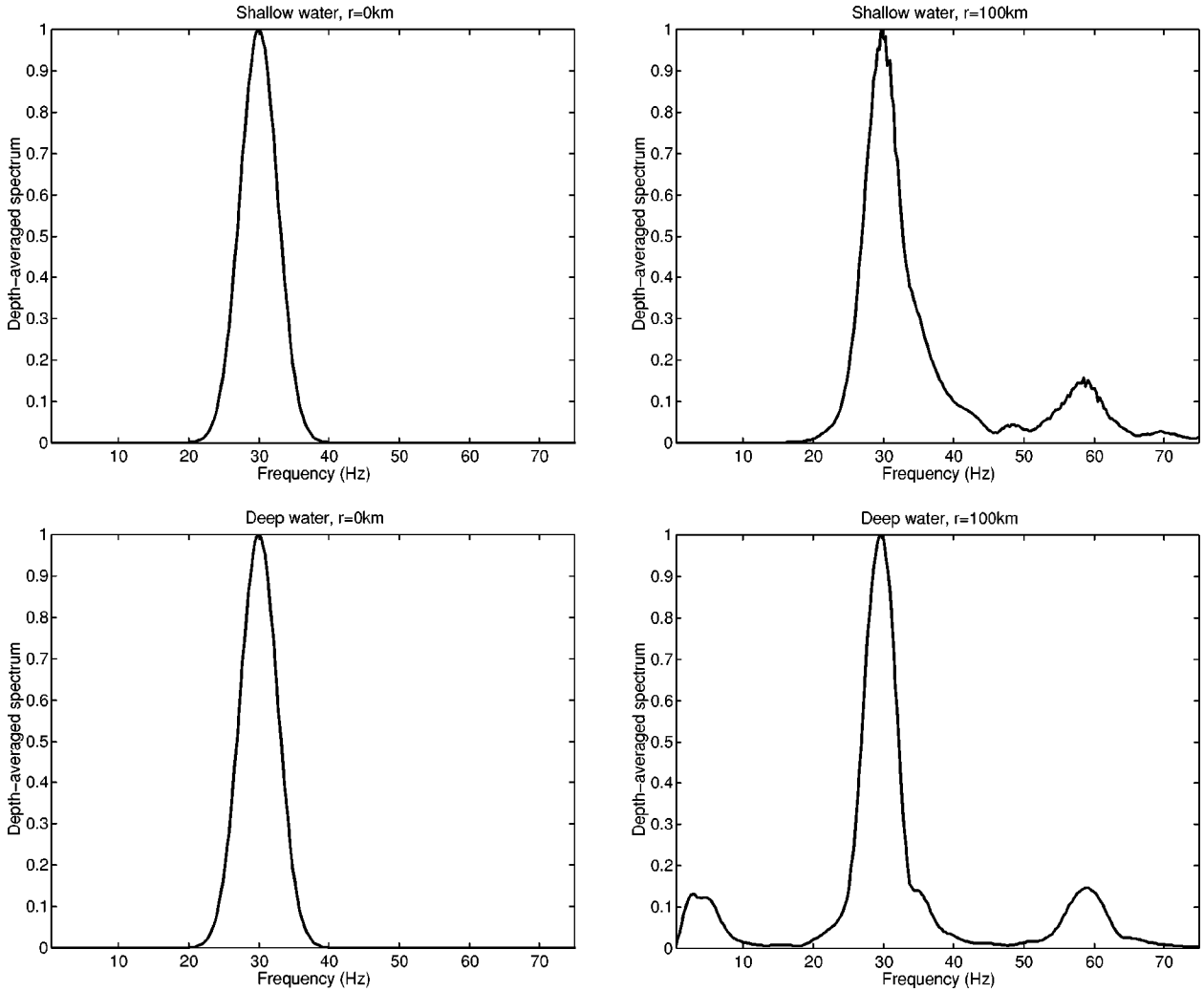

FIG. 4. Normalized depth-averaged spectrum in shallow and deep water for a narrowband source centered at $f_c = 30$ Hz, with a maximum overdensity $R_m = 5 \times 10^{-3}$, at 0 and 100-km ranges.

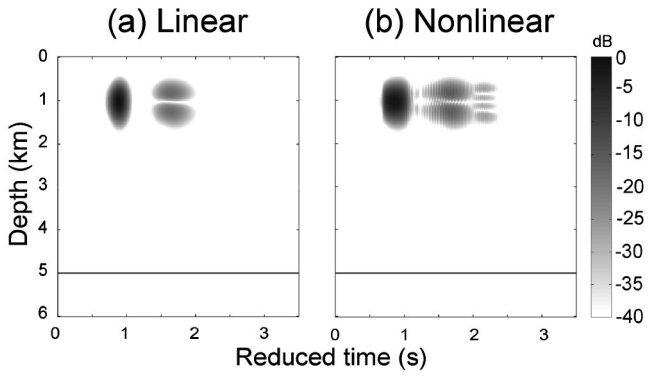

FIG. 5. Time series envelopes in deep water at 3000-km range, for a narrowband source centered at $f_c = 30$ Hz, at 100 m depth in shallow water, with a maximum overdensity $R_m = 1 \times 10^{-5}$ (a. linear case) and $R_m = 5 \times 10^{-3}$ (b. nonlinear case).

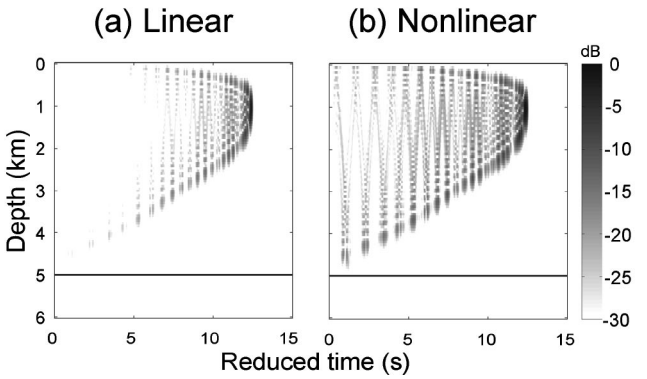

FIG. 6. Time series envelopes in deep water at 3000-km range, for a narrowband source centered at $f_c = 30$ Hz, at 800 m depth in deep water, with a maximum overdensity $R_m = 1 \times 10^{-5}$ (a. linear case) and $R_m = 5 \times 10^{-3}$ (b. nonlinear case).

width. A narrow frequency band source creates a narrow low-frequency peak, whereas a shorter duration source signal would generate a broader low-frequency spectrum. Figure 4(b) shows that this parametric low-frequency peak is truncated in shallow water, since it is below the waveguide cutoff frequency.

For finite-amplitude sound waves, nonlinear effects develop at short ranges. One of our aims in this study is to determine some characteristics at very long ranges of such waves that originate from nonlinear wave propagation. After an initial distance in which the nonlinear wave loses energy to shock processes and increased bottom penetration,[11] its amplitude is sufficiently low so that its interaction with the waveguide becomes essentially linear. Then, a linear normal mode code can be used to study the modal decomposition of the acoustic field and also propagate it to much longer ranges (i.e., several thousand km). Even though the presence of nonlinearity does not lend itself to a straightforward representation in linear normal modes, similarities between the two cases are expected since the nonlinearities are weak.

At the 100-km range, the field is spectrally decomposed into its modal components before the linear code KRAKEN can carry out the propagation to longer ranges frequency by frequency and mode by mode.[8,23] These modal components at very long ranges are finally synthesized into signal arrivals in the time domain. For the range-dependent environment [Fig. 1(b)], the adiabatic approximation is used in the linear normal modes propagation. Figure 5 represents the time series envelopes, for linear and nonlinear propagation paths in this case, at a 3000-km range, after propagation in deep water. Figure 6 represents the time series envelopes for linear and nonlinear cases, at a 3000-km range, when the source is placed in deep water at a source depth $z_s = 800$ m.

B. Influence of the environment on dispersion of modes

Figures 7(a) and 7(b) represent the group speed versus phase speed, at the center frequency $f = 30$ Hz, respectively for the shallow and deep water waveguides (Fig. 1). The lower-order modes correspond to the lower grazing angles and thus the lower phase speeds. Group speeds correspond to time of arrivals for a given range. In shallow water, the lower-order modes travel faster [Fig. 7(a)]. In deep water [Fig. 7(b)], the dispersion of modes is mainly due to refraction: the group-speed order of the lower-order modes is flipped in comparison to the shallow water case [Fig. 7(a)].

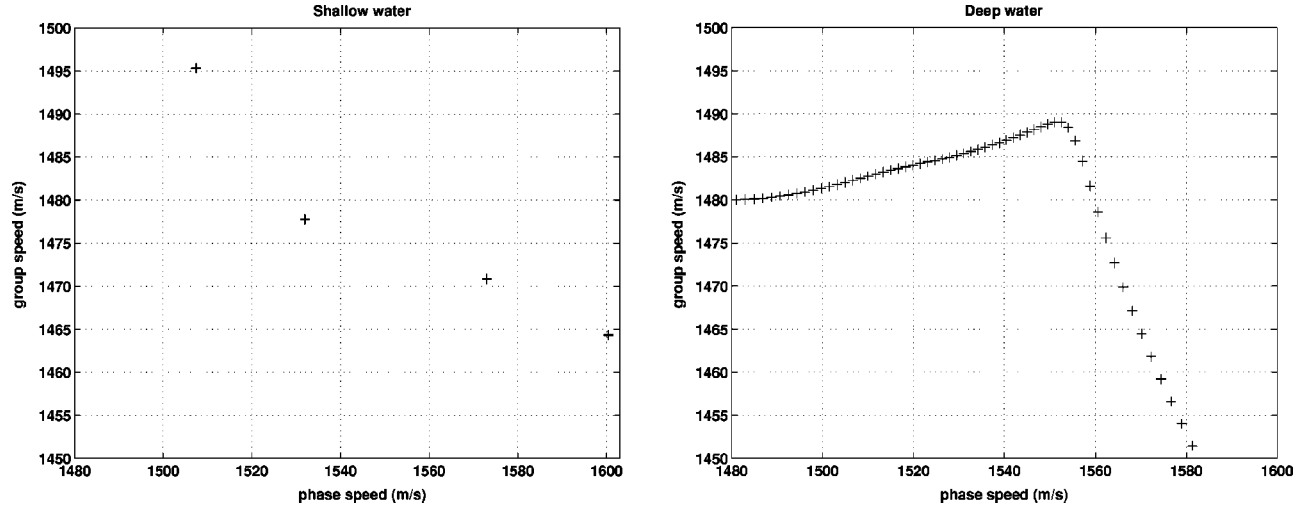

FIG. 7. Group speed vs phase speed at the central source frequency $f = 30$ Hz for shallow and deep water.

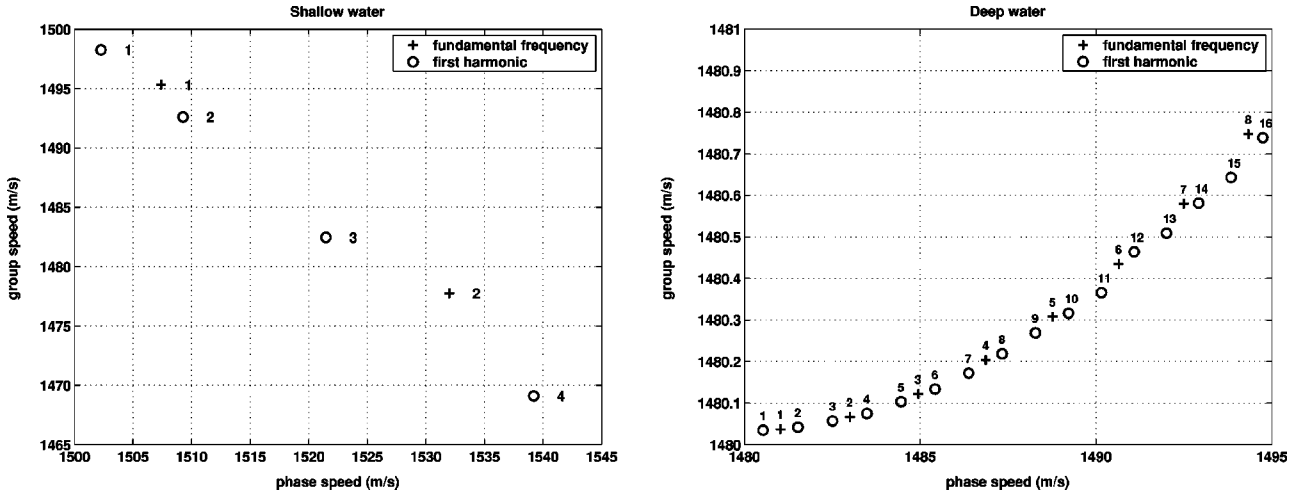

FIG. 8. Group speed vs phase speed, for the central source frequency $f=30$ Hz and the first harmonic $f=60$ Hz, for shallow and deep water. The numbers display the indexes of the lower order modes that are excited.

So, the higher-order modes travel faster in deep water, which is clearly visible on a greatly dispersed signal (Fig. 6 at a 3000-km range). Figure 5 shows that when the signal is propagated to deep water after the 100-km range, the lower-order modes still arrive first at the 3000-km range because only a few modes are excited in shallow water, and the group speeds of these lowest-order modes are almost the same in deep water [Fig. 7(b)]. Indeed, the difference between the group speed for the first mode and the third mode is approximately 25 m/s in shallow water [Fig. 7(a)] and about 0.08 m/s in deep water [Fig. 7(b)]. In shallow water the modes are expected to be separated in time faster than in deep water. Then, for the shallow-to-deep water case, the dispersion of modes mainly occurs in shallow water and the signal keeps approximately the same shape along several hundred kilometers when it propagates in the deep water SOFAR channel (Fig. 5). Note that, at long ranges, even if the time separation of modes is larger in shallow water, the total time spread of the signals will be much larger in deep water than in shallow water since more modes are excited. In shallow water, due to a strong interaction with the bottom, the higher-order modes are attenuated and only few modes survive.

C. Nonlinear effects on modal distribution

Finite-amplitude sound waves interact differently with the ocean/bottom interface than linear waves because of the nonlinear contribution to the local sound speed. The dispersion of a nonlinear pulse is therefore expected to be different from that of a linear pulse. Two differences can be observed between linear and nonlinear propagation: the first one is related to the energy redistributed among modes and the second concerns the modal arrival time. In both environments, the energy initially carried by the source frequency components is redistributed to the other frequencies created by nonlinear effects.

Figures 2 and 5 show that, for a shallow water source, the nonlinear signature results in low-order mode attenuation due to shock formation: the nonlinearities lead to more relative energy for higher-order modes, which are left after the initial mode stripping due to the bottom interaction. When the nonlinearities are strong enough, there is a tendency toward energy equipartition at long ranges leading to an arrival time structure in lower-order modes characterized by an almost uniform weight for each mode. This modal equipartition results from mode coupling at short ranges, where the nonlinearities are sufficiently high and the modes are not dispersed. Figure 8(a) shows, for the modes that are mainly excited (Figs. 2 and 5), the group speed versus phase speed at the fundamental frequency and at the first harmonic. In shallow water, the individual modes at the first harmonic travel faster than the ones at the fundamental. Note that the modes associated with the nonlinear frequency components are excited during propagation. It is expected that an optimum in nonlinear mode excitation is reached at the shock wave formation distance. The phase lag then induced could slightly influence the arrival time of the nonlinear modes by delaying the time separation of modes. But the difference in group speeds between the fundamental and first harmonic, as explained before [Fig. 8(a)], is primarily responsible for the difference between linear and nonlinear arrival time structure. Figure 9 shows the mode amplitudes versus frequency for the linear and nonlinear cases in shallow water at 100-km range showing that the first harmonic leads to an excitation of modes 3 and 4. According to the previous comments, the

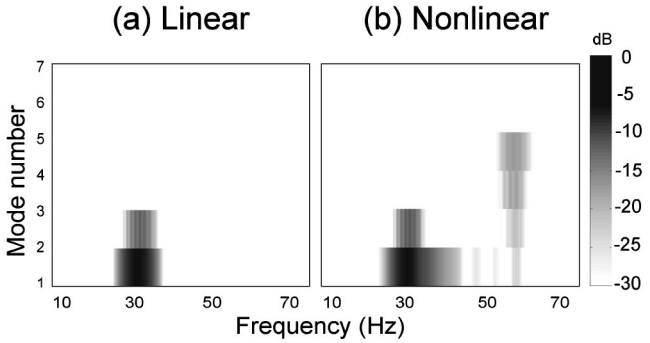

FIG. 9. Mode amplitudes (dB) versus mode-number and frequency, in shallow water at 100 km for a narrowband source centered at $f_c=30$ Hz, with a maximum overdensity $R_m=1\times10^{-5}$ (a. linear case) and $R_m=5\times10^{-3}$ (b. nonlinear case).

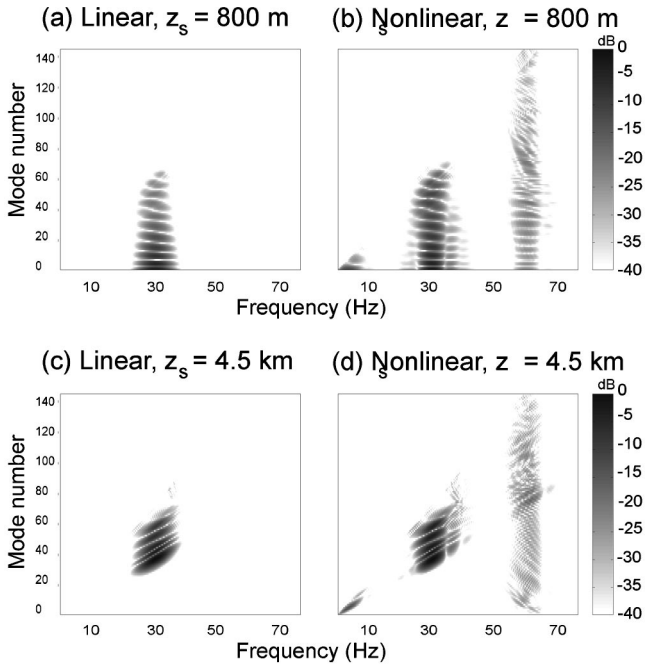

FIG. 10. Mode amplitudes (dB) versus mode-number and frequency, in deep water, for linear (left) and nonlinear (right) for two different source depths [($z_s = 800$ (top) and $z_s = 4.5$ km (bottom)].

nonlinear modes (modes 3 and 4 at 60 Hz) arrive just after the first linear modes (modes 1 and 2 at 30 Hz), respectively (Fig. 2). This example illustrates what we mean by frequency–mode coupling.

D. Influence of parametric mode conversion on sea/bottom coupling

A recent study[24] has reported that sound speed fluctuations due to internal waves are a dominant source of mode coupling in long-range propagation scenarios. Internal-wave-induced scattering eventually results in an equipartition of energy among the lower-order modes in deep water. Also, a broadening of the signals[25] is attributable to the exchange of energy among the modes, caused by the internal waves. Acoustic normal mode propagation is strongly nonadiabatic due to internal waves.[26] The results presented previously (Sec. II C) show that, due to a mode coupling induced by a frequency redistribution of the acoustic energy, the impact of nonlinearities also leads to a result that displays a tendency toward an equipartition and a mixed arrival time structure of the modes. In this section, even if the results presented are still limited to ocean propagation and sources in the ocean, we point out a particular effect of frequency–mode coupling that is an increased sea/bottom coupling.

Figure 10 represents the mode amplitudes versus frequency at a 100-km range for the 5-km deep water waveguide for two source depths ($z_s = 800$ m and $z_s = 4.5$ km) and for linear and nonlinear cases. The number of propagating modes increases with frequency. When the source is at the SOFAR axis ($z_s = 800$ m), all the modes are excited. Whereas if the source is near the bottom ($z_s = 4.5$ km), the SOFAR trapped modes are not excited. Then, in the linear case, only the highest-order modes are excited and propagate over long ranges (Fig. 10). Figure 10 shows that, in a nonlinear case, mode coupling at short ranges leads to an excitation of the lowest-order modes due to parametric low-frequency generation. Even when the source is close to the bottom (Fig. 10 for $z_s = 4.5$ km), the nonlinearities induce low-order mode excitation that contributes to increased bottom penetration.

We have shown that parametric low-frequency generation also increases the sea/bottom coupling. For a wave originating from the earth, we expect to obtain sufficiently high acoustic amplitudes in the water, and consequently, find similar qualitative results to the ones presented here based on a source in the water above the bottom: nonlinearities would redistribute energy toward lower frequencies, and then, more penetrating modes would be excited, leading to increased sea/bottom coupling. Consequently, such nonlinear effects may be involved in the processes of conversion of seismic waves to (and from) acoustic energy, which can result in the efficient excitation of T waves by seismic sources located inland or by underground explosions. From a terrestrial origin, T waves are acoustic energy trapped in the SOFAR channel that can propagate efficiently over a long distance without significant energy loss. Understanding the nature of the coupling between the underwater acoustic field and the land seismic field is important for evaluating the performance of the hydroacoustic stations attempting to detect nuclear explosions.[1,27] The seismic T-wave conversion process at the ocean bottom is not well understood. Two different mechanisms have been identified to explain the T-wave coupling.[28] The first one is ''slope conversion,'' which is controlled by seafloor slope.[29,30] The second mechanism is scattering of energy into the sound channel at bathymetric promontories in close proximity to the source region. This ''seafloor scattering'' is then dominated by the seafloor depth.[31,32] Figure 10 shows that the nonlinearities induce energy transfer toward low-order modes at the parametric difference frequency. These low-order modes excite the water column and interact with the bottom. Consequently, this phenomenon could be responsible for T-wave generation.

IV. CONCLUSION

Nonlinear characteristics of long-range acoustic paths in shallow and deep water environments have been demonstrated in this paper. The results illustrate that nonlinear properties modify the spectral evolution of the acoustic field and its modal distribution. A nonlinear birthmark may therefore be present in hydroacoustic signals recorded at long distance related to underwater explosions. This study should contribute to diagnosing the nonlinear origin of such signals.

In shallow water, the acoustic field is altered by the waveguide interfaces earlier than in deep water, inducing lower geometrical spreading. Hence, the nonlinear effects on acoustical propagation are greater if an explosion occurs in shallow water. In deep water, the lowest-order modes have roughly the same group speed. Therefore, the shallow-to-deep water time series still display an arrival time structure with the lower-order modes arriving first in contrast to the deep water case.

Nonlinearities can lead to similar results to those obtained for long-range ocean acoustic wave propagation in random media: a tendency to have an equipartition of lower-order modes. Finally, the nonlinear process of parametric conversion of bottom interacting modes to lower-order SOFAR trapped modes suggests a potential mechanism for T-wave generation. In summary, after long-range propagation, it may be possible to characterize a strong explosion by studying the remaining low-frequency waves generated by parametric interaction.

ACKNOWLEDGMENTS

This research was sponsored by Defense Threat Reduction Agency, Contract No. DTRA01-00-C-0084.

[1] P. Gerstoft, ''Assessment of hydroacoustic processing in the CTBT release one monitoring software,'' Comprehensive Nuclear-Test-Ban-Treaty Organisation, Vienna, Austria, 1999. http://www-mpl.ucsd.edu/people/gerstoft/

[2] G. L. D'Spain, W. A. Kuperman, J. Orcutt, and M. Hedlin, ''Long range localisation of impulsive sources in the atmosphere and ocean from focus regions in single element spectrograms,'' *Proceedings of the 22nd*, Annual Seismic Research Symposium, 2000.

[3] P. H. Rogers, ''Weak-shock solution for underwater explosive shock waves,'' J. Acoust. Soc. Am. **62**, 1412–1419 (1977).

[4] N. R. Chapman, ''Measurement of the waveform parameters of shallow explosive charges,'' J. Acoust. Soc. Am. **78**, 672–681 (1985).

[5] N. R. Chapman, ''Source levels of shallow explosive charges,'' J. Acoust. Soc. Am. **84**, 697–702 (1988).

[6] T. L. Geers and K. S. Hunter, ''An integrated wave-effects model for an underwater explosion bubble,'' J. Acoust. Soc. Am. **111**, 1584–1601 (2002).

[7] B. E. McDonald and W. A. Kuperman, ''Time-domain formulation for pulse propagation including nonlinear behavior at a caustic,'' J. Acoust. Soc. Am. **81**, 1406–1417 (1987).

[8] M. Porter, The KRAKEN normal mode program, SACLANTCEN SM-245, La Spezia, Italy, 1991.

[9] B. E. McDonald, ''High-angle formulation for the nonlinear progressive-wave equation model,'' Wave Motion **31**, 165–171 (2000).

[10] B. E. McDonald, ''Nonlinear effects in source localization,'' *Ocean Acoustic Interference Phenomena*, edited by W. A. Kuperman and G. L. D'Spain (American Institute of Physics, Melville, NY, 2002).

[11] J. J. Ambrosiano, D. Plante, B. E. McDonald, and W. A. Kuperman, ''Nonlinear propagation in an ocean waveguide,'' J. Acoust. Soc. Am. **87**, 1473–1481 (1990).

[12] J. E. White, *Seismic Waves* (McGraw-Hill, New York, 1965).

[13] X. Zabolotskaya and X. Khokhlov, ''Quasi-plane waves in the nonlinear acoustics of confined beams,'' Sov. Phys. Acoust. **15**, 35–40 (1969).

[14] V. P. Kuznetsov, ''Equations of nonlinear acoustics,'' Sov. Phys. Acoust. **16**, 467–470 (1971).

[15] P. Blanc-Benon, B. Lipkens, L. Dallois, M. F. Hamilton, and D. T. Blackstock, ''Propagation of finite amplitude sound through turbulence: Modeling with geometrical acoustics and the parabolic approximation,'' J. Acoust. Soc. Am. **111**, 487–498 (2002).

[16] K. Castor, B. E. McDonald, and W. A. Kuperman, ''Equations of nonlinear acoustics and weak shock propagation,'' *16th International Symposium on Nonlinear Acoustics*, Moscow, Russia, 2002.

[17] B. E. McDonald, ''High order upwind flux methods for scalar hyperbolic conservation laws,'' J. Comput. Phys. **56**, 448–460 (1984).

[18] M. F. Hamilton and D. T. Blackstock, *Nonlinear Acoustics* (Academic, New York, 1998).

[19] P. J. Westervelt, ''Parametric acoustic array,'' J. Acoust. Soc. Am. **35**, 535–537 (1963).

[20] B. K. Novikov, O. V. Rudenko, and V. I. Timochenko, ''Nonlinear underwater acoustics,'' ASA, New York, 1987.

[21] J. Marchal, ''Acoustique non linéaire: contribution théorique et expérimentale à l'étude de l'émission paramétrique,'' Ph.D. dissertation, Université Pierre et Marie Curie-Paris 6, 2002.

[22] C. Barrière and D. Royer, ''Diffraction effects in the parametric interaction of acoustic waves: Application to measurements of the nonlinearity parameter B/A in liquids,'' IEEE Trans. Ultrason. Ferroelectr. Freq. Control **48**, 1706–1715 (2001).

[23] F. B. Jensen, W. A. Kuperman, M. B. Porter, and H. Schmidt, *Computational Ocean Acoustics* (American Institute of Physics, Springer-Verlag, New York, NY, 1994).

[24] K. E. Wage, A. B. Baggeroer, and J. C. Preisig, ''Modal analysis of broadband acoustic receptions at 3515-km range in the North Pacific using short-time fourier techniques,'' J. Acoust. Soc. Am. **113**, 801–817 (2003).

[25] J. A. Colosi, S. M. Flatte, and C. Bracher, ''Internal-wave effects on 1000-km oceanic acoustic pulse propagation: Simulation and comparison with experiment,'' J. Acoust. Soc. Am. **96**, 452–468 (1994).

[26] J. A. Colosi and the ATOC group, ''A review of recent results on ocean acoustic wave propagation in random media: Basin scales,'' IEEE J. Ocean. Eng. **24**, 138–155 (1999).

[27] G. L. D'Spain, L. P. Berger, W. A. Kuperman, J. L. Stevens, and G. E. Baker, ''Normal mode composition of earthquake T phases,'' Pure Appl. Geophys. **158**, 475–512 (2001).

[28] C. H. Li, ''T-waves excited by S-waves and oscillated within the ocean above the southeastern taiwan forearc,'' Geophys. Res. Lett. **28**, 3297–3300 (2001).

[29] J. Talandier and E. A. Okal, ''On the mechanism of conversion of seismic waves to and from T-waves in the vicinity of island shores,'' Bull. Seism. Soc. Am. **88**, 621–632 (1998).

[30] P. F. Piserchia, J. Virieux, D. Rodrigues, S. Gaffet, and J. Talandier, ''Hybrid numerical modelling of T-wave propagation: application to the mid-plate experiment,'' Geophys. J. Int. **133**, 789–800 (1998).

[31] C. D. de Groot-Hedlin and J. A. Orcutt, ''Excitation of T-phases by seafloor scattering,'' J. Acoust. Soc. Am. **109**, 1944–1954 (2001).

[32] C. D. de Groot-Hedlin and J. A. Orcutt, ''T-phase observation in northern california: Acoustic to seismic coupling at a weakly elastic boundary,'' Pure Appl. Geophys. **158**, 513–530 (2001).